IEEE Access
Multidisciplinary | Rapid Review | Open Access Journal

Received July 11, 2019, accepted July 17, 2019, date of publication July 22, 2019, date of current version August 6, 2019.

Digital Object Identifier 10.1109/ACCESS.2019.2930121

Reducing PAPR With Low Complexity for 4G and 5G Waveform Designs

YASIR AMER AL-JAWHAR[1,5], KHAIRUN NIDZAM RAMLI[1], AIDA MUSTAPHA[2], SALAMA A. MOSTAFA[2], NOR SHAHIDA MOHD SHAH[3], AND MONTADAR ABAS TAHER[4]

[1]Faculty of Electrical and Electronic Engineering, Universiti Tun Hussein Onn Malaysia, Parit Raja 86400, Malaysia
[2]Faculty of Computer Science and Information Technology, Universiti Tun Hussein Onn Malaysia, Parit Raja 86400, Malaysia
[3]Faculty of Engineering Technology, Universiti Tun Hussein Onn Malaysia, Parit Raja 84600, Malaysia
[4]Department of Communications Engineering, College of Engineering, University of Diyala, Baqubah 32001, Iraq
[5]Iraqi Ministry of Communications, Baghdad 10012, Iraq

Corresponding author: Yasir Amer Al-Jawhar (free_cccc@yahoo.com)

This work was supported by the Universiti Tun Hussein Onn Malaysia Vot under Grant E15501.

ABSTRACT Partial transmit sequence (PTS) technique is considered as one of the efficient methods to reduce the high peak-to-average power ratio (PAPR) problem in 4G waveform design such as the orthogonal frequency division multiplexing (OFDM) systems. Filtered-OFDM (F-OFDM) is a new candidate in the 5G waveform development with maintaining a high level of commonality with legacy OFDM systems, but the high PAPR value is still a considerable problem because F-OFDM supports the orthogonal transmission. Although the PTS technique improves the PAPR reduction performance significantly, the high computational complexity level for optimizing the phases of the transmitting signal restricts this technique in practical applications. Therefore, the low computational complexity level of the PTS technique leads to the adoption of this technique for PAPR reduction in the multicarrier systems such as OFDM and F-OFDM. In this paper, a new low complexity algorithm (Gray-PF-PTS) by combining the Gray code and the left feedback shift register operation based on a specific mapping rule has been proposed. The numerical results indicate that the Gray-PF-PTS algorithm extensively reduces the computational complexity level without degradation the PAPR reduction performance compared with the conventional PTS method. Furthermore, the OFDM and F-OFDM systems based on the Gray-PF-PTS algorithm have been compared regarding the PAPR, bit error rate (BER), and power spectrum density (PSD) performances.

INDEX TERMS OFDM, F-OFDM, 4G, 5G, PAPR, PTS.

I. INTRODUCTION

As one of the most attractive techniques in high-data-rate communication, the orthogonal frequency division multiplexing (OFDM) systems are considered a popular waveform design for many wireless communication standards. OFDM has many promising features such as high immunity against multipath fading [1], easy implementation using the Inverse Fast Fourier Transform (IFFT) algorithm [2], and high capacity [3]. Consequently, the OFDM system has been adopted by many wireless communication standards such as Wireless Personal Area Networks (WPAN) IEEE 802.15 [4], Wireless Local Area Network (WLAN) IEEE.802.11 [5], Wireless Metropolitan Area Networks (WMAN) IEEE.802.16 [6], and 4G-Long-Term Evaluation (4G-LTE) standard [7]. However, OFDM is restricted by some obstacles such as the high peak-to-average-power ratio (PAPR), signaling synchronization, and high spectral leakage [8]. The high PAPR value of the transmitted signals is considered the major drawback of the OFDM system, which drives the OFDM signals to work in the nonlinear region of high-power amplifier (HPA) and this leads to appearing undesirable degradation in the Bit Error Rate (BER) performance [9].

Recently, the fifth generation (5G) applications such as Internet of Things (IoT), Machine to Machine (M2M) communications, and high-speed mobile networks have been introduced to meet the rapid growth of the communication markets [10], [11]. Accordingly, several waveform candidates such as Filtered-OFDM (F-OFDM), Universal

The associate editor coordinating the review of this manuscript and approving it for publication was Debashis De.

Filtered Multi-Carrier (UFMC), and Filter Bank Multi-Carrier (FBMC) have been suggested to meet the requirements of the 5G technology [12], [13]. Among various advanced candidates, F-OFDM scheme is receiving increasing attention in the 5G waveform development, due to its promising advantages such as suppressing Out-Of-Band Emission (OOBE), supporting the orthogonal transmission, improving the spectral efficiency, supporting asynchronous transmission, low latency and maintaining high level of commonality with legacy OFDM systems [14], [15]. However, the high PAPR value is still a considerable problem because F-OFDM supports the orthogonal transmission, and the transmitter filter reduces the mean power of the signal which increases the PAPR value.

To avoid the large PAPR value in OFDM signals, various methods for PAPR reduction have been suggested, such as clipping and filtering [16], companding [17], constellation extension [18], Selective Level Mapping (SLM) [19], and Partial Transmit Sequence (PTS) [20]. Among all existing techniques, PTS is very promising because of its efficient PAPR reduction performance without any signal distortion. Unfortunately, PTS has a high computational complexity level for finding the OFDM sequence with the lowest PAPR value because the conventional PTS (C-PTS) needs an exhaustive search over all combinations of allowed phase rotation factors and its complexity increases exponentially with the number of subblocks [21]. Selecting the suitable elements of weighting phase factor is very interesting for an efficient implementation, where $\{\pm 1\}$ or $\{\pm 1, \pm \mathrm{j}\}$ of the elements phase factors leads the system to avoid the complicated multiplication operations. But, the PAPR reduction performance is directly proportional to the number of elements phase weighting factors [9].

In the literature, several algorithms have been focused on reducing the computational complexity level in the PTS technique. In [22], Liu *et al.* introduced phase adjustment PTS algorithm for reducing the complexity calculations depending on a predetermined angle to update the phase factors for a certain number of iterations. Liu's algorithm has lower complexity than C-PTS, but this leads to degradation in the PAPR performance. In [23], Lan-Xun and Li-Bin presented a low complexity algorithm by combining the m-sequence code with PTS. The phase factors of Lan's algorithm are generated based on mapping the m-sequence code into $\{\pm 1, \pm \mathrm{j}\}$ elements. Hence, the computational complexity is reduced at the expense of degradation in PAPR reduction performance. In addition, Jayalath and Telebureau [24] proposed a new tactic for reducing the computational complexity by setting a threshold value of PAPR, and then the candidate signal which falls below the threshold value is chosen for transmission. Jayalath's algorithm reduces the number of iterations for finding the optimum phase rotation factors, but the cost is retraction in the PAPR performance. Furthermore, a low computation complexity algorithm was proposed by Wang and Liu [21] based on grouping the partitioned subblocks and then each group is optimized by using the same set of phase factors. Wang's algorithm reduces the computational complexity better than C-PTS without degradation in the PAPR performance. In the same manner, Kim [25] applied cyclic shift to reduce the computational complexity in PTS technique, while the algorithms in [26]–[29] reduced the computational complexity relatively based on $\{\pm 1, \pm \mathrm{j}\}$. Lastly, Junjun *et al.* [30] presented another approach for reducing the computational complexity by employing Gray code nature to produce the phase rotation factors. The key point of Junjun's algorithm is to make use of a Gray code and the inherent relationship between the phase factor sequences; with the consideration that the weighting factors are constrained based on $\{\pm 1\}$. The Junjun method can achieve PAPR reduction performance almost the same as the C-PTS method based on $\{\pm 1\}$. However, the computational complexity is reduced significantly.

Based on the literature, it is clear that there is a trade-off between the PAPR reduction performance and the computational complexity level in the PTS technique. Hence, the high computational complexity level restricts the PTS technique in the practical applications. In this paper, a new phase weighting algorithm for PTS named Gray phase factor PTS (Gray-PF-PTS) has been proposed, which aims to reduce computational complexity and achieve almost the same performance in PAPR reduction compared to C-PTS based on $\{\pm 1, \pm \mathrm{j}\}$. In the Gray-PF-PTS algorithm, the Gray code inherent relationship is employed to generate the phase rotation factors by adding the code string with the Left Feedback Shift Register (LFSR) operation through a specific mapping rule. Moreover, the proposed algorithm can be expanded into three algorithms Gray-PF-PTS A, Gray-PF-PTS B, and Gray-PF-PTS C in order to enhance the PAPR reduction performance. The computational complexity level based on Gray-PF-PTS algorithm is reduced dramatically compared with C-PTS. Most importantly, the Gray-PF-PTS algorithms have a lower number of side information bits than the C-PTS method.

This paper is organized as follows. In Section II, we discuss the basic concept of the OFDM and F-OFDM systems. Section III presents an analysis of the conventional PTS technique. Section IV introduces the proposed algorithm. In Section V, the performances of the proposed algorithms based on the simulation and numerical results are discussed. Finally, we end the paper with brief conclusions in Section.

II. OFDM AND F-OFDM SYSTEMS

In the OFDM framework, the input data sequence $X_k = \{k = 0, 1, 2, \ldots, N-1\}$ is mapped by one of the constellation mapping techniques such as Quadrate Amplitude Modulation (QAM), where N denotes the number of the subcarriers. The baseband signal is converted from the serial into the parallel and then the IFFT block is applied to modulate the baseband signal with N subcarriers orthogonality. The discrete OFDM signal $x(n)$ in the time-domain can be described

as [31]

$$x(n) = \frac{1}{\sqrt{N}} \sum_{k=0}^{N-1} X_k e^{j2\pi k \frac{n}{N}}, \quad \text{n} = 0, 1, ..., \text{N} - 1, \quad (1)$$

where $j = \sqrt{-1}$. After that, the cycle prefix (CP) insertion is implemented to the OFDM signal to prevent the signal from the Inter-Symbol-Interference (ISI) [32]. Therefore, the OFDM signal is generated by the superposition of the N sub-carriers with the samples of the baseband signal. Accordingly, when the phases of these samples are in high consistency, the instantaneous power of some samples may be added together and become much higher than the mean power of the signal. Hence, PAPR has defined as the maximum peak power of the OFDM signal divided by the mean power [33]. The PAPR is measured in decibel (dB), and it can be expressed by [34]

$$\text{PAPR} = \frac{\max|x(n)|^2}{E\{|x(n)|^2\}}, \quad (2)$$

where $E\{.\}$ is the mean value of the signal. In addition, to get the accurate PAPR calculations, the baseband signal is sampled multiple times the Nyquist rate (oversampling operation). The oversampling operation is performed by inserting $(L\text{-}1)N$ zeros between the baseband samples in the frequency domain, where L represents the oversampling factor. Moreover, to evaluate the PAPR reduction level in the OFDM system, the Complementary-Cumulative-Distribution-Function (CCDF) is usually used, where CCDF represents the probability of the PAPR value that exceeds a certain threshold value ($PAPR_0$) [3]

$$\Pr(\text{PAPR} > PAPR_0) = 1 - (1 - \text{e}^{(-PAPR_0)})^{NL}. \quad (3)$$

As mentioned earlier, F-OFDM is considered as one of the waveform candidates in the 5G technology, where the F-OFDM system depends on filtering the whole bandwidth of the OFDM signal before transmitting. The transceiver structure of F-OFDM is depicted in Figure 1. In the transmitter side, the transmitter generates its OFDM signal together with cyclic prefixes, and then the F-OFDM signal is obtained by passing the OFDM signal through an appropriately designed spectrum shaping filter $f(n)$. In this case, the transmitter filter $f(n)$ bandwidth is equal to the total frequency width of the assigned subcarriers for the OFDM signal. At the receiver side, the received signal is first passed to the receiver filter $f*(-n)$, which is matched to the transmitter filter (spectrum shaping filter) [35]. The resulting signal is then passed through the regular OFDM receiver as depicted in Figure. 1. The receiver filter works to isolate the received signal from any contributions of the neighboring signals. Hence, the receiver filter is to ensure that the received signal is passed through the next stage without interference from the adjacent signals [36]. The added filters in F-OFDM increase the complexity of the system. Also, the transmitter filter works to increase the PAPR value of the F-OFDM system because the added filter in the transmitter leads to increasing power

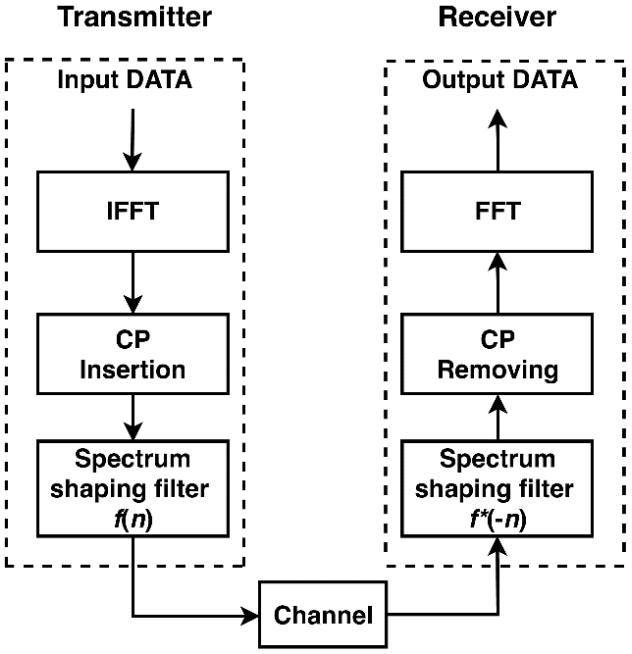

FIGURE 1. F-OFDM block diagram.

distribution among the samples and then the mean power of the signal is reduced. Therefore, the F-OFDM system has a PAPR value higher than that of the OFDM system.

On the other hand, the filter design involves the trade-off between the time and frequency domain characteristics, and it is also associated with the implementation complexity. Hence, filter design plays an important role in the F-OFDM system. The ideal low pass filter (LPF) is a sinc function, where its impulse response is a suitable spectrum shaping with time windowing mask to provide a good time localization and to ensure the smooth transitions for both ends [37], [38]. Therefore, choosing a suitable window function can accomplish a flexible trade-off between the frequency and time localization. Thus, the ISI value can be reduced to an acceptable level. The Rooted Raised Cosine (RRC) window function works to meet the requirement of the flexibility in F-OFDM better than other window functions such as Remez and Hanning [14]. Therefore, the time response of the RRC window filter is expressed as [39]

$$w_{RRC}(n) = \left[0.5\left(1 + cos\left(\frac{2\pi n}{FL - 1}\right)\right)\right]^{\alpha}, \quad (4)$$

where FL symbolizes the filter length, and α stands for the roll-off factor which is the parameter that controls the window shape, and it is limited to $0 < \alpha < 1$. The roll-off factor of the RRC window works to provide additional freedom to achieve a balance between frequency and time localization [39]. In the F-OFDM system, the filter length is allowed to exceed the cyclic prefix length to fulfill more flexibility for design and to achieve the better balance between the frequency and time localization [40]. In contrast, the filter

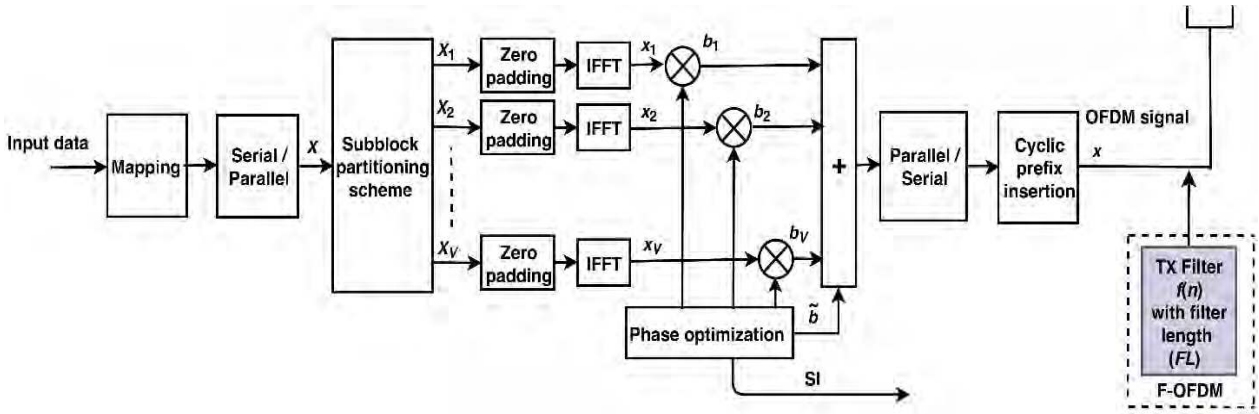

FIGURE 2. C-PTS block diagram (Transmitter side) [41].

length is sensitive with the complexity of the system, where long filter length increases the complexity. Hence, the filter length in the F-OFDM system should be limited to a certain length. In general, the benefits promised by F-OFDM need properly designed filters.

III. CONVENTIONAL PTS METHOD

The C-PTS strategy has been viewed as a probabilistic scenario for reducing the high PAPR pattern in the OFDM system. In other words, the C-PTS method can improve PAPR reduction performance without destroying the OFDM signal. In contrast, the high computational complexity is the prominent drawback of the C-PTS method, because the system should perform a comprehensive search for finding the optimum phase factor [41]. The C-PTS method depends on two essential stages to improve the PAPR reduction performance; the subblock partitioning schemes and optimizing the phase factors in the subblocks. There are three conventional partitioning schemes in C-PTS, Interleaving partitioning (IL-PTS), Adjacent partitioning (Ad-PTS), and Pseudo-random partitioning (PR-PTS) [3]. The PTS method works to improve PAPR reduction performance without destroying the OFDM signal depending on multiple signal representations. In other words, multiple copies will be individually processed in parallel to find the minimum PAPR of the signal. Hence, PTS is a guarantee that output PAPR is minimum. Also, the phase rotation factors used in the time domain in the PTS technique works to reduce the high consistency of the multicarrier samples in the OFDM signal by changing the phases of these samples, thus the PAPR value of the OFDM signal is reduced accordingly. Figure 2 depicts the principle idea of the C-PTS method, where the input data sequence X is partitioned by one of the partitioning schemes into several subblocks as follow

$$X = \sum_{v=1}^{V} X_v, \tag{5}$$

where V represents the number of subblocks. Next, the subblocks are multiplied by a set of the unity amplitude phase factor. After that, the N-IFFT is applied to modulate the data samples with the subcarriers, and then to transform the data from the frequency domain into the time domain. The linear property of the IFFT is exploited to transform the phase rotation factors into the time domain. Therefore, the discrete time domain signal can be expressed as [20]

$$x = \text{IFFT}\{\sum_{v=1}^{V} b_v X_v\} = \sum_{v=1}^{V} b_v \text{IFFT}\{X_v\}, \tag{6}$$

where b_v $\{v = 1, 2, \ldots, V\}$ denotes to phase rotation factors. Afterward, the transformed subblocks in the time domain are rotated with the set of phase factors to produce a group of the candidate signals named partial transmit sequences (pts_s). Lastly, the PAPR values of pts_s are calculated, and the candidate that achieved the lowest PAPR value is chosen for transmitting. Therefore, the OFDM signal can be written as [31]

$$\text{OFDM signal} = \sum_{v=1}^{V} \tilde{b}_v x_v, \tag{7}$$

where $\tilde{b}_v$ represents the optimum phase rotation factor. In addition, the elements of the weighting factors are usually fixed to dodge the complex multiplications, so the phase factors are limited to $\{\pm 1\}$ or $\{\pm 1, \pm \text{j}\}$. Therefore, the weighting factors vector can be expressed as [41]

$$b_v = e^{j2\pi v/W} | v = \{0, 1, \ldots\ldots, W1\}, \tag{8}$$

where W represents the number of allowed phase rotation factors. Moreover, the optimum phase weighting factor that achieves the lowest PAPR value is obtained by

$$\tilde{b}_v = \underset{1 \le w \le W}{\arg\min} \left(\underset{0 \le n \le NL-1}{\max} \left| \sum_{v=1}^{V} b_v x_v \right| \right), \tag{9}$$

where arg min (.) represents a global minimum value based on the phase rotation factors.

In the C-PTS method, W^{V-1} of repetitions must be examined for finding the optimum phase rotation factor; with the

consideration that the first element of the weighting factors $b1$ is fixed to 1 without any loss of performance [42]. This operation imposes a heavy burden on the system. Hence, the main limitation of the conventional PTS technique is the high computational complexity for finding the optimum phase factors. It is equally important to note that the index of the optimum phase rotation factor should be sent to the receiver as Side Information (SI) in order to recover the original data. Therefore, the number of SI bits in the C-PTS method can be expressed as [43]

$$\mathrm{SI}^{\text{C-PTS}} = \log_2 W^{V-1} \text{bits per symbol.} \tag{10}$$

On the other hand, the computational complexity of the C-PTS method in the time domain is the number of complex additions ($C_{\text{add}}^{\text{C-PTS}}$) and complex multiplications ($C_{\text{mult}}^{\text{C-PTS}}$) that required for optimizing the phases of the transformed sub-blocks and can be expressed as [44]

$$C_{\text{add}}^{\text{C-PTS}} = W^{V-1} \times N \times (V-1), \tag{11}$$

and,

$$C_{\text{mult}}^{\text{C-PTS}} = W^{V-1} \times N \times (V+1). \tag{12}$$

In the F-OFDM system, the computational complexity in the time-domain is higher than that of the OFDM system, because the transmitter filter imposes extra complexity on the system. The computational complexity in F-OFDM is held by multiplying the OFDM signal with the filter length. Therefore, the number of complex additions in the F-OFDM system is similar to the OFDM system, while the number of complex multiplications of the F-OFDM system is increased based on the filter length [45]. Therefore, the number of complex multiplications of the F-OFDM system in the time-domain can be expressed as

$$C_{\text{mult/F-OFDM}}^{\text{C-PTS}} = C_{\text{mult/OFDM}}^{\text{C-PTS}} + \text{Filter complexity}, \tag{13}$$

then,

$$C_{\text{mult/F-OFDM}}^{\text{C-PTS}} = W^{V-1} \times N \times (V+1) + [N \times (FL-1)]. \tag{14}$$

In general, the PTS technique is considered as an effective method for improving the PAPR reduction performance in both OFDM and F-OFDM systems. In contrast, the computational complexity restricts the C-PTS technique in practical applications because finding the optimum phase rotation factor imposes a heavy burden on the system. Therefore, the gain for the PAPR reduction performance in the PTS technique will be at the expense of increasing in the system complexity.

IV. THE PROPOSED ALGORITHM

The PTS technique is a probabilistic technique (multiple signal representations). In other words, multiple copies will be individually processed in parallel to find the minimum PAPR of the signal. Hence, PTS is a guarantee that output PAPR is minimum. The proposed technique as it has been shown follows up the same approach. The key idea of the Gray-PF-PTS algorithms is to generate phase rotation factors depending on the Gray code strings with the LFSR operation through a specific mapping rule. The conventional PTS technique performs an extensive search for finding the optimum phase rotation factor to weigh the transformed subblocks depending on the number of subblocks and the scope of phase factors. Hence the C-PTS examines W^{V-1} iterations to find the optimum phase factors and this imposes a heavy burden on the system especially when the scope of the phase factors W is $\{\pm 1, \pm \mathrm{j}\}$. In contrast, the proposed algorithm reduces the number of iterations for finding the optimum phase factors into 2^V vectors depending on the relationship of the generated vectors by Gray code with LFSR operation. Hence, the computational complexity level of the system is significantly reduced. Moreover, the proposed algorithm is expanded into three algorithms A, B, and C to improve the PAPR reduction performance, where the PAPR reduction performance is directly proportional with the number of candidate signal that generated by phase factors. Therefore, the proposed algorithms exploit the relationship between the phase rotation vectors to reduce the computational complexity level of the PTS technique without degrading the PAPR reduction performance.

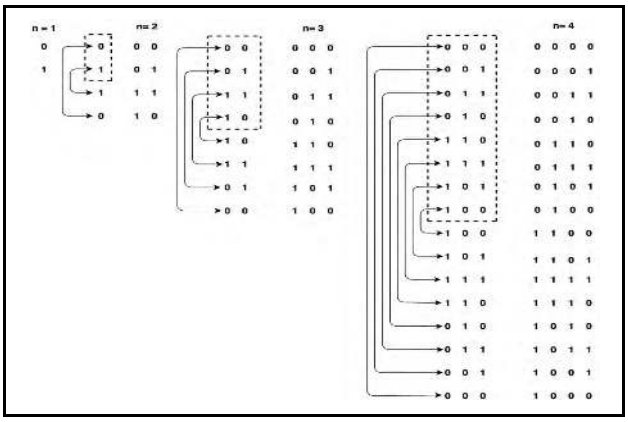

FIGURE 3. Gray code (n = 4).

In this subsection, a new algorithm called Gray-PF-PTS algorithm is introduced to decrease the number of iterations for finding the optimum phase factor. The procedure of Gray-PF-PTS algorithm relies on employing Gray code to generate the phase rotation factors by adding the code string with the LFSR operation through a specific mapping rule [46], [47]. Moreover, the proposed algorithm can be expanded into three algorithms Gray-PF-PTS A, Gray-PF-PTS B, and Gray-PF-PTS C in order to improve the PAPR reduction performance.

The Gray code is a reflected code, in which the code strings for (n) bits can be created recursively from the code strings of (n-1) bits by reflecting this code strings in reverse order. In such a way, prefixing the original code strings are assigned by a binary 0, and prefixing the reflected code strings by a binary 1. After that, the original code strings list is combined with the reflected code strings list to generate the final list of the Gray code. Figure 3 illustrates the Gray code string based on four bits.

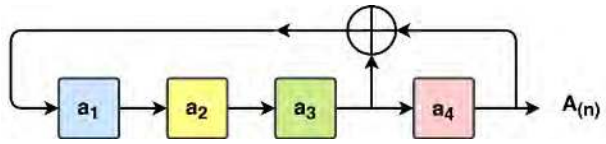

FIGURE 4. LFSR operation [48].

LFSR operation		Inverting the codeword begins with '0'	
Original bits	New bits	Original bits	New bits
0 0 0 0 →	0 0 0 0	1 1 1 1	1 1 1 1
0 0 0 1 →	1 0 0 0	1 1 1 0	1 0 0 0
0 0 1 1 →	0 0 0 1	1 1 0 0	1 1 1 0
0 0 1 0 →	1 0 0 1	1 1 0 1	1 0 0 1
0 1 1 0 →	1 0 1 1	1 0 0 1	1 0 1 1
0 1 1 1 →	0 0 1 1	1 0 0 0	1 1 0 0
0 1 0 1 →	1 0 1 0	1 0 1 0	1 0 1 0
0 1 0 0 →	0 0 1 0	1 0 1 1	1 1 0 1
1 1 0 0 →	0 1 1 0	1 1 0 0	1 0 0 1
1 1 0 1 →	1 1 1 0	1 1 0 1	1 1 1 0
1 1 1 1 →	0 1 1 1	1 1 1 1	1 0 0 0
1 1 1 0 →	1 1 1 1	1 1 1 0	1 1 1 1
1 0 1 1 →	1 1 0 1	1 0 1 1	1 1 0 1
1 0 1 1 →	0 1 0 1	1 0 1 1	1 0 1 0
1 0 0 1 →	1 1 0 0	1 0 0 1	1 1 0 0
1 0 0 0 →	0 1 0 0	1 0 0 0	1 0 1 1

FIGURE 5. Codewords generation.

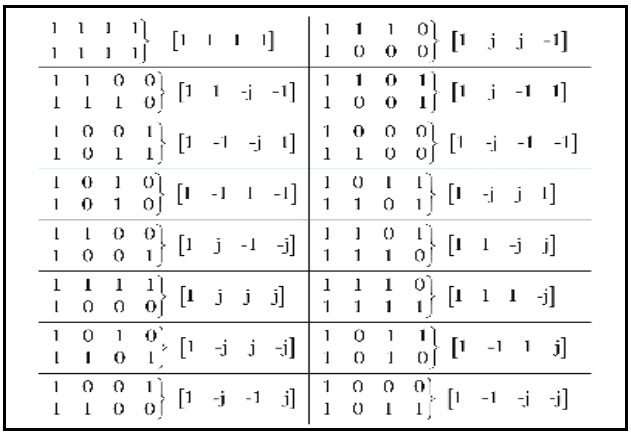

FIGURE 6. Phase rotation factor vectors generation.

TABLE 1. The phase rotation factors in the Gray-PF-PTS A algorithm.

A	B	C	D
[1, 1, 1, 1]	[1, -1, -j, 1]	[1, j, -1, 1]	[1, -j, -1, 1]
[1, 1, 1, -j]	[1, -1, -j, -j]	[1, j, -1, -j]	[1, -j, -1, -j]
[1, 1, -j, -1]	[1, -1, 1, -1]	[1, j, j, -1]	[1, -j, j, -1]
[1, 1, -j, j]	[1, -1, 1, j]	[1, j, j, j]	[1, -j, j, j]

In short, the key idea of the Gray-PF-PTS algorithms is to generate phase rotation factors depending on the Gray code strings; these algorithms can be used when the scope of the phase factors W is $\{\pm 1, \pm j\}$.

A. GRAY-PF-PTS A ALGORITHM

In this case, the phase rotation factors are generated based on performing LFSR operation to each codeword in the Gray code list to create a new codeword. The LFSR operation is to sum the last two bits of the codeword using Modulo-2 to generate the first bit of the new codeword, and then immediately makes feedback shift to the left, while the remaining bits execute a standard shift register [48], as shown in Figure 4.

Besides, the two codewords (the original codeword and the created codeword from LFSR) are summed together depending on the mapping rule that is: $1 + 1 = 1$, $0 + 0 = -1$, $1 + 0 = j$, $0 + 1 = -j$; with the consideration that inverting the whole binary string that begins with "0" to ensure the first element of the phase rotation factor equals always 1. Therefore, the number of generated phase rotation factors is (2^V) vectors, which can be used to rotate the transformed subblocks in the time domain. For instance, when the number of subblocks $V = 4$ and the number of bits in each codeword of the Gray code $n = 4$, thus the Gray code list consists of $2^V = 16$ codewords, as shown in Figure 3. After that, each codeword performs the LFSR operation to generate a new codeword, and then the codewords that begin with "0" are inverted (it is marked in yellow) to ensure all the codewords in each list begin with "1", as depicted in Figure 5.

Afterword, each couple of the codewords in the last list is summed depending on the mapping rule, as shown in Figure 6.

Finally, Table 1 shows the list of generated phase rotation factor vectors from the Gray-PF-PTS A algorithm which is utilized to rotate the transformed subblocks in the time domain and then to generate (2^V) candidate signals.

Accordingly, the phase rotation factors can be divided into 4 groups, and the elements in each group are consistent in a fixed structure, in which the first column is always (1), and the fourth element of the first row is always (1). Hence, the number of multiplication and addition operations can be reduced based on the relationship between the phase factors in each group as follow:

B. MULTIPLICATION OPERATIONS

- The first column always consists of element 1, so there is no need to perform any multiplication operation.
- The second column consists of the same elements, so there is only one multiplication operation.
- The third column consists of two different elements, so there are two of the multiplication operations.
- The fourth column consists of three different elements, so there are three of the multiplication operations.

As a result, each group will perform 6 of the multiplication operations instead of 16 of the multiplication operations in C-PTS, as shown in Table 2. Therefore, the number of

TABLE 2. The multiplication operations in the Gray-PF-PTS A algorithm.

A	B	C	D
[1, 1, 1, 1]	[1, -1, -j, 1]	[1, j, -1, 1]	[1, -j, -1, 1]
[1, 1, 1, -j]	[1, -1, -j, -j]	[1, j, -1, -j]	[1, -j, -1, -j]
[1 , 1 , -j , -1]	[1, -1, 1, -1]	[1, j, j, -1]	[1, -j, j, -1]
[1 , 1 , -j , j]	[1, -1, 1, j]	[1, j, j, j]	[1, -j, j, j]

TABLE 3. The addition operations in the Gray-PF-PTS A algorithm.

A	B	C	D
[1 , 1 , 1, 1]	[1, -1, -j, 1]	[1, j, -1, 1]	[1, -j, -1, 1]
[1 , 1 , 1 , -j]	[1, -1, -j, -j]	[1, j, -1, -j]	[1, -j, -1, -j]
[1 , 1 , -j , -1]	[1, -1, 1, -1]	[1, j, j, -1]	[1, -j, j, -1]
[1 , 1 , -j , j]	[1, -1, 1, j]	[1, j, j, j]	[1, -j, j, j]

multiplication operations for Gray-PF-PTS A is written as

$$C_{\text{mult}}^{\text{Gray-PTS A}} = 2^{V-1} \times \left(\frac{V}{2} + 3\right) \times N, \quad W = \{\pm 1, \pm \text{j}\}. \quad (15)$$

C. ADDITION OPERATIONS

In each group, every two vectors will be considered together to calculate the number of complex additions, as follow

- The first row performs three of the addition operations.
- The second row performs only one addition operation.
- The third row performs three of the addition operations.
- The fourth row performs only one addition operation.

As a result, each group will perform 8 addition operations instead of 12 addition operations in C-PTS, as shown in Table 3. Therefore, the number of addition operations of Gray-PF-PTS A can be calculated as

$$C_{\text{add}}^{\text{Gray-PTS A}} = 2^{V-1} \times V \times N, W = \{\pm 1, \pm \text{j}\}. \quad (16)$$

Gray-PF-PTS A algorithm can reduce the computational complexity significantly compared with the C-PTS technique, especially when $W = \{\pm 1, \pm \text{j}\}$. However, the PAPR reduction performance will record some degradation, because the number of candidates will be reduced.

D. THE GRAY-PF-PTS B ALGORITHM

In this case, additional phase rotation factors are generated based on performing the conjugate operation to each phase rotating vector of the Gray-PF-PTS A list. Hence, a new set of the phase rotation factored will be created, as shown in Table 4.

Accordingly, the phase rotation factors can be divided into 4 groups, and the elements in each group are consistent in a fixed structure, in which all the vectors have j and -j elements except the vectors [1, 1, 1, 1], and [1, −1, 1, −1]; thus, they will be ignored, because they already existed in the Gray-PF-PTS A list. Therefore, the number of multiplication and

TABLE 4. The phase rotation factors in the Gray-PF-PTS B algorithm.

A	B	C	D
[1, 1, 1, 1]	[1, -1, j, 1]	[1, -j, -1, 1]	[1, j, -1, 1]
[1, 1, 1, j]	[1, -1, j, j]	[1, -j, -1, j]	[1, j, -1, j]
[1, 1, j, -1]	[1, -1, 1, -1]	[1, -j, -j, -1]	[1, j, -j, -1]
[1, 1, j, -j]	[1, -1, 1, -j]	[1, -j, -j, -j]	[1, j, -j, -j]

TABLE 5. The multiplication operations in the Gray-PF-PTS B algorithm.

A	B	C	D
[1 , 1 , 1 , 1]	[1 , -1 , j , 1]	[1, -j, -1, 1]	[1, j, -1, 1]
[1 , 1 , 1 , j]	[1 , -1 , j , j]	[1, -j, -1, j]	[1, j, -1, j]
[1 , 1 , j , -1]	[1 , -1 , 1 , -1]	[1, -j, -j, -1]	[1, j, -j, -1]
[1 , 1 , j , -j]	[1 , -1 , 1 , -j]	[1, -j, -j, -j]	[1, j, -j, -j]

addition operations can be reduced based on the relationship between the phase factors in each group, as follow:

E. MULTIPLICATION OPERATIONS

All the groups will follow the same procedure of the Gray-PF-PTS A algorithm except groups A and B.

Group A

- The first column always consists of element 1, so there is no need to perform any multiplication operation.
- The second column consists of the same elements, so there is only one multiplication operation.
- The third column consists of two different elements, so there are two of the multiplication operations.
- The fourth column consists of three different elements, so there are three of the multiplication operations.

Group B

- The first column always consists of element 1, so there is no need to perform any multiplication operation.
- The second column consists of the same elements, so there is only one multiplication operation.
- The third column consists of two different elements, so there are two of the multiplication operations.
- The fourth column consists of two different elements, so there are two of the multiplication operations.

As a result, each group will perform 6 of the multiplication operations except group B which has 5 of the multiplication operations, as shown in Table 5. Therefore, the number of multiplication operations of using the conjugate operation can be calculated as

$$C_{\text{mult}}^{\text{conjugate}} = \left[2^{V-1}\left(\frac{V}{2} + 3\right) \times N\right] - 3N. \quad (17)$$

Hence, the number of multiplication operations of the Gray-PF-PTS B algorithm can be calculated as

$$C_{\text{mult}}^{\text{Gray-PTS B}} = C_{\text{mult}}^{\text{Gray-PTS A}} + C_{\text{mult}}^{\text{conjugate}}, \quad (18)$$

TABLE 6. The addition operations in the Gray-PF-PTS B algorithm.

A	B	C	D
[1 , 1 , 1 , 1]	[1 , -1 , j , 1]	[1, -j, -1, 1]	[1, j, -1, 1]
[1 , 1 , 1 , j]	[1 , -1 , j , j]	[1, -j, -1, j]	[1, j, -1, j]
[1 , 1 , j , -1]	[1 , -1 , 1 , -1]	[1, -j, -j, -1]	[1, j, -j, -1]
[1 , 1 , j , -j]	[1 , -1 , 1 , -j]	[1, -j, -j, -j]	[1, j, -j, -j]

thus,

$$C_{\text{mult}}^{\text{Gray-PTS B}} = 2\left[2^{V-1}\left(\frac{V}{2}+3\right)\times N\right] - 3N, \quad W = \{\pm 1, \pm \text{j}\}. \tag{19}$$

F. ADDITION OPERATIONS

All the groups will follow the same procedure of the Gray-PF-PTS A algorithm except groups A and B.

Group A

- The second row performs three of the addition operations.
- The third row performs three of the addition operations.
- The fourth row performs only one addition operation.

Group B

- The first row performs three of the addition operations.
- The second row performs only one addition operation.
- The fourth performs three of the addition operations.

As a result, each group will perform 8 addition operations except two of the groups will perform 7 addition operations, as shown in Table 6. Therefore, the number of addition operations using the conjugate operation can be calculated as

$$C_{\text{add}}^{\text{conjugate}} = \left[2^{V-1} \times V \times N\right] - 2N, \tag{20}$$

thus,

$$C_{\text{add}}^{\text{Gray-PTS B}} = 2\left[2^{V-1} \times V \times N\right] - 2N, \quad W = \{\pm 1, \pm \text{j}\}. \tag{21}$$

The Gray-PF-PTS B algorithm can reduce the computational complexity significantly compared with C-PTS technique, especially when $W = \{\pm 1, \pm \text{j}\}$. Moreover, the PAPR reduction performance will improve better than the Gray-PF-PTS A algorithm, because the number of candidates will be increased.

G. THE GRAY-PF-PTS C ALGORITHM

In this case, an additional list of the phase rotation factors is generated based on performing the flipping operation to the fourth's element of each phase rotating vector in the Gray-PF-PTS A list. Hence, a new set of the phase rotation factor will be created, as shown in Table 7.

Accordingly, the phase rotation factors can be divided into 4 groups, and the elements in each group is consistent in a fixed structure, in which the fourth element of the third row

TABLE 7. The phase rotation factors in the Gray-PF-PTS C algorithm.

A	B	C	D
[1 , 1 , 1 , -1]	[1 , -1 , -j , -1]	[1, j, -1, -1]	[1, -j, -1, -1]
[1 , 1 , 1 , j]	[1 , -1 , -j , j]	[1, j, -1, j]	[1, -j, -1, j]
[1 , 1 , -j , 1]	[1 , -1 , 1 , 1]	[1, j, j, 1]	[1, -j, j, 1]
[1 , 1 , -j , -j]	[1 , -1 , 1 , -j]	[1, j, j, -j]	[1, -j, j, -j]

is always (1), and the vectors [1, 1, 1, j] and [1, −1, 1, −j] will be ignored, because they already existed in the Gray-PF-PTS A list. Therefore, the number of the multiplication and addition operations can be reduced based on the relationship between the phase factors in each group, as follow:

H. MULTIPLICATION OPERATIONS

All the groups will follow the same procedure of the Gray-PF-PTS A algorithm except groups A and B, as follow

- The first column always consists of element 1, so there is no need to perform any multiplication operation.
- The second column consists of the same elements, so there is only one multiplication operation.
- The third column consists of two different elements, so there are two of the multiplication operations.
- The fourth column consists of two different elements, so there are two of the multiplication operations.

As a result, each group will perform 6 multiplication operations except group A and B will perform 5 multiplication operations, as shown in Table 8. Therefore, the number of multiplication operations of flipping operation can be calculated as

$$C_{\text{mult}}^{\text{flipping}} = \left[2^{V-1}\left(\frac{V}{2}+3\right)\times N\right] - 4N. \tag{22}$$

TABLE 8. The multiplication operations in the Gray-PF-PTS C algorithm.

A	B	C	D
[1 , 1 , 1 , -1]	[1 , -1 , -j , -1]	[1, j, -1, -1]	[1, -j, -1, -1]
[1 , 1 , 1 , j]	[1 , -1 , -j , j]	[1, j, -1, j]	[1, -j, -1, j]
[1 , 1 , -j , 1]	[1 , -1 , 1 , 1]	[1, j, j, 1]	[1, -j, j, 1]
[1 , 1 , -j , -j]	[1 , -1 , 1 , -j]	[1, j, j, -j]	[1, -j, j, -j]

Hence, the number of the multiplication operations of Gray-PF-PTS C algorithm can be calculated as

$$C_{\text{mult}}^{\text{Gray-PTS C}} = C_{\text{mult}}^{\text{Gray-PTS A}} + C_{\text{mult}}^{\text{Gray-PTS B}} + C_{\text{mult}}^{\text{flipping}}, \tag{23}$$

thus,

$$C_{\text{mult}}^{\text{Gray-PTS C}} = 3\left[2^{V-1}\left(\frac{V}{2}+3\right)\times N\right] - 7N, \quad W = \{\pm 1, \pm \text{j}\}. \tag{24}$$

TABLE 9. The addition operations in the Gray-PF-PTS C algorithm.

A	B	C	D
[1 , 1 , 1 , -1]	[1 , -1 , -j , -1]	[1, j, -1, -1]	[1, -j, -1, -1]
[1 , 1 , 1 , j]	[1 , -1 , -j , j]	[1, j, -1, j]	[1, -j, -1, j]
[1 , 1 , -j , 1]	[1 , -1 , 1 , 1]	[1, j, j, 1]	[1, -j, j, 1]
[1 , 1 , -j , -j]	[1 , -1 , 1 , -j]	[1, j, j, -j]	[1, -j, j, -j]

I. ADDITION OPERATIONS

All the groups will follow the same procedure of the Gray-PF-PTS A algorithm except groups A and B

Group A

- The first row performs three of the addition operations.
- The third row performs three of the addition operations.
- The fourth row performs only one addition operation.

Group B

- The first row performs three of the addition operations.
- The second row performs only one addition operation.
- The fourth performs three of the addition operations.

As a result, each group will perform 8 addition operations except two of the groups will perform 7 addition operations, as shown in Table 9. Therefore, the number of addition operations of using the flipping operation can be calculated as

$$C_{\text{add}}^{\text{flipping}} = \left[2^{V-1} \times V \times N\right] - 2N, \tag{25}$$

Hence, the number of the addition operations of Gray-PF-PTS C algorithm can be calculated as

$$C_{\text{add}}^{\text{Gray-PTS C}} = C_{\text{add}}^{\text{Gray-PTS A}} + C_{\text{add}}^{\text{Gray-PTS B}} + C_{\text{add}}^{\text{flipping}}, \tag{26}$$

thus,

$$C_{\text{add}}^{\text{Gray-PTS C}} = 3\left[2^{V-1} \times V \times N\right] - 4N, \quad W = \{\pm 1, \pm \text{j}\}. \tag{27}$$

The Gray-PF-PTS C algorithm can reduce the computational complexity significantly compared with C-PTS technique, especially when $W = \{\pm 1, \pm \text{j}\}$. Moreover, the PAPR reduction performance will be almost the same that of the C-PTS method, because the number of candidates will be increased.

In brief, the Gray-PTS algorithms when $W = \{\pm 1, \pm \text{j}\}$ are summarized as follows:

i. Perform Gray code for $\text{n} = V$.
ii. Perform LFSR for each codeword of Gray code list.
iii. Invert the codewords that begin with (0).
iv. Add each codeword with corresponding LFSR codeword depending on the mapping pattern.
v. Collect the generated phase rotation factor vectors and apply the Gray-PF-PTS A algorithm.
vi. Perform the conjugate operation on the Gray-PF-PTS A algorithm to generate a new list of the phase rotation factors and apply the Gray-PF-PTS B algorithm
vii. Perform the flipping operation to the Gray-PF-PTS A algorithm to generate an additional list of the phase rotation factors and apply the Gray-PF-PTS C algorithm.

On the other hand, the Gray-PF-PTS algorithm has another advantage compared with the C-PTS method, where the side information bits required to recover the original signal can be reduced. In the three types of the Gray-PTS algorithm, it can only transfer the Gray code index to the receiver and then producing the phase rotation factor of the three types of the Gray-PF-PTS algorithms according to the LFSR or conjugate or flipping operation. Therefore, the number of side information bits of the Gray-PF-PTS algorithms can be given as

$$\text{SI}^{\text{Gray-PTS}} = \log_2 2^V, \quad W = \{\pm 1, \pm \text{j}\}. \tag{28}$$

V. RESULTS AND DISCUSSION

The key idea of the Gray-PF-PTS algorithm is to employ the Gray code strings to produce the phase rotation factors for optimizing the transformed subblocks and then to combine these subblocks to generate the candidate signals. In this subsection, the CCDF will be evaluated when $W = \{\pm 1, \pm \text{j}\}$, $N = 512$ and 4096 points, while the order of QAM constellation mapping (M) is 256 and 64, respectively. In addition, the oversampling factor $L = 4$, the number of the subblocks $V = 4$, the number of cyclic prefixes (CP) is 7% of the IFFT length, and the filter length FL is the half of IFFT length +1, and the roll-off factor of the RRC window α is 0.6. The Solid-State Power Amplifier (SSPA) nonlinear HPA model which is commonly used in mobile and cellular communication systems has been adopted. In this simulation, the amplifier parameters are computed when Input Back-Off (IBO = 3 dB), and the smoothness control (p = 3.286) [49].

Moreover, the three types of the Gray-PF-PTS algorithm will be applied to the OFDM and F-OFDM systems to evaluate the PAPR reduction performance and the BER level. It important to mention that the C-PTS method is assumed based on a pseudo-random partitioning scheme, so as the conventional PTS is termed to PR-PTS in this simulation.

A. PAPR AND BER EVALUATION

In the OFDM system, the number of subcarriers is chosen as 512 and $M = 256$, these parameters correspond to IEEE802.11.ac standard, 4G-LTE standard, and 5G candidate for the wireless systems. In this part, the PAPR reduction performance of the proposed algorithms and some of the improved PTS algorithm in literature are simulated, where the proposed algorithms Gray-PF-PTS A, Gray-PF-PTS B, and Gray-PF-PTS C when $V = 4$ and $W = 4$ represent 16, 30, and 40 iterations. Besides, the conventional PTS method, PR-PTS, ($W = 4$), Liu's algorithm ($W = 4$) [22], Lanxun's algorithm ($W = 4$) [23], Jayalath's algorithm (8.6 dB threshold) [24], L. Wang's algorithm ($W = 4$) [21], Junjun's algorithm ($W = 2$) [30], and PR-PTS ($W = 2$) represent 64, 30, 12, 38, 64, 8, and 8 iterations. As can be seen from

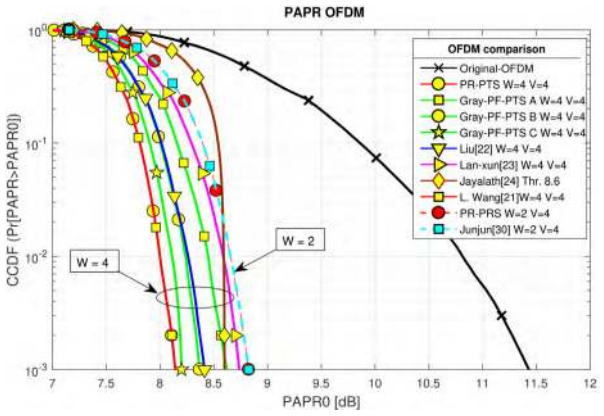

FIGURE 7. CCDF of the Gray-PF-PTS algorithms in OFDM, $N = 512$, $M = 256$.

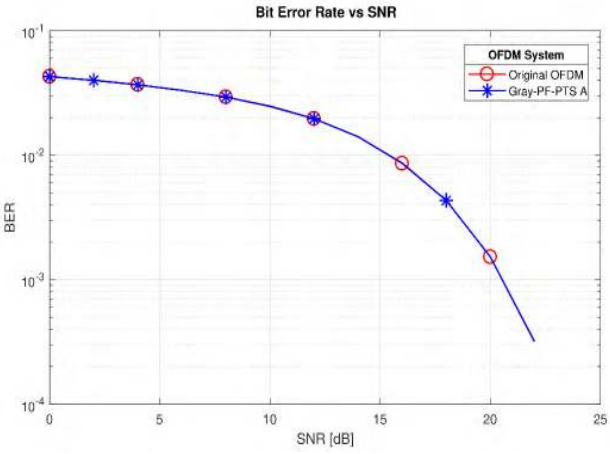

FIGURE 8. BER of the Gray-PF-PTS A algorithm in OFDM, $N = 512$, $M = 256$.

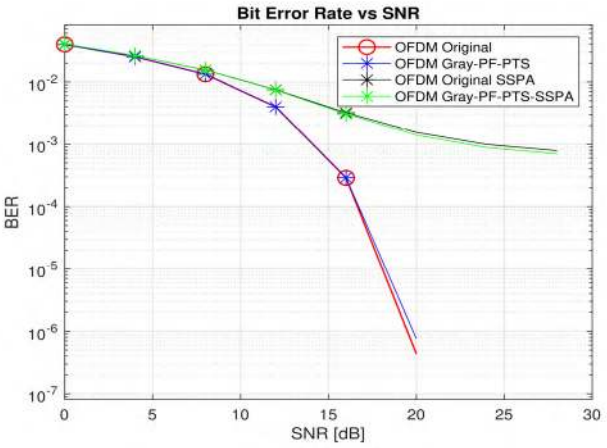

FIGURE 9. BER of the Gray-PF-PTS A algorithm in OFDM with and without SSPA, $N = 512$, $M = 64$.

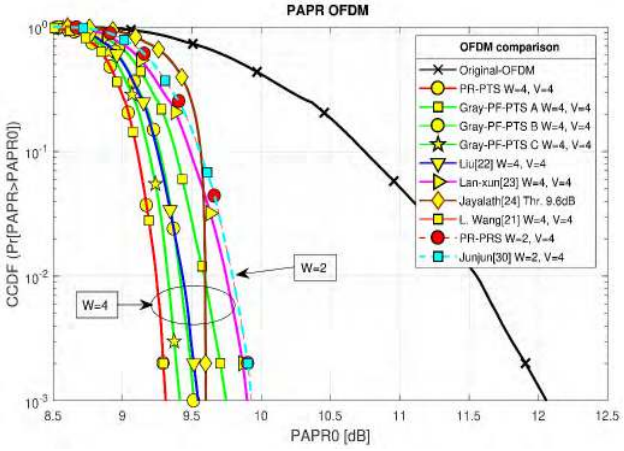

FIGURE 10. CCDF for the Gray-PF-PTS algorithm in OFDM, $N = 4096$, $M = 64$.

Figure 7, when CCDF at 10^{-3}, the Gray-PF-PTS A, Gray-PF-PTS B, and Gray-PF-PTS C algorithms reduce the PAPR value compared with the original OFDM signal by 2.81 dB, 3.07 dB, 3.23 dB, respectively. Also, PR-PTS, Liu's algorithm, Lan-xun's algorithm, Jayalath's algorithm, L. Wang's algorithm reduce the PAPR value compared to the original OFDM signal by 3.29 dB, 3.02 dB, 2.7 dB, 2.83 dB, and 3.29 dB, respectively. In the same hand, the PR-PTS ($W = 2$) method and the Junjun algorithm reduce the PAPR value compared to the original signal by 2.61 dB. It is clear that the Gray-PF-PTS C achieves almost the same PAPR value compared to the PR-PTS ($W = 4$) method; with the consideration that the Gray-PF-PTS C only needs 40 iterations to achieve its PAPR value, while the PR-PTS method performs 64 iterations. On the other hand, Figure 8 presents the BER performance of the Gray-PF-PTS A algorithm compared with the original OFDM signal. The result indicates that the BER performance for both signals is identical, because of the probabilistic nature of the Gray-PF-PTS A algorithm, which maintains the BER performance without degradation. Moreover, Figure 9 illustrates the BER performance of the Gray-PF-PTS A with and without HPA (SSPA). The nonlinearity exhibits of the HPA distortion causes a loss of orthogonality among the subcarriers, and this leads to in-band distortion or intercarrier interference (ICI) is introduced [50]. The ICI power is proportional to the amplitude of the signal at the amplifier input and this causes a considerable BER degradation.

In the same manner, another simulation is conducted when the IFFT size is 4096, and the constellation order is 64-QAM, see Figure 10. The results show that the PAPR value has been reduced using Gray-PF-PTS A, Gray-PF-PTS B, and Gray-PF-PTS C algorithms by 2.3 dB, 2.54 dB, and 2.64 dB. Moreover, the PAPR value has been reduced using PR-PTS ($W = 4$), Liu's algorithm ($W = 4$), Lan-xun's algorithm, Jayalath's algorithm (9.6 dB threshold), L. Wang's algorithm, PR-PTS ($W = 2$), and Junjun's algorithm by 2.74 dB, 2.51 dB, 2.15 dB, 2.45 dB, 2.74 dB, 2.12 dB, and 2.12 dB, respectively. Therefore, the Gray-PF-PTS C algorithm can achieve almost the same PAPR reduction performance of the PR-PTS ($W = 4$) method with fewer iterations, and this

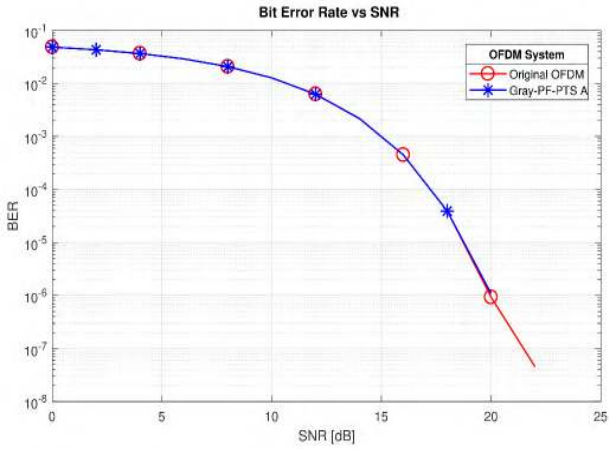

FIGURE 11. BER of the Gray-PF-PTS A algorithm in OFDM, $N = 4096$, $M = 64$.

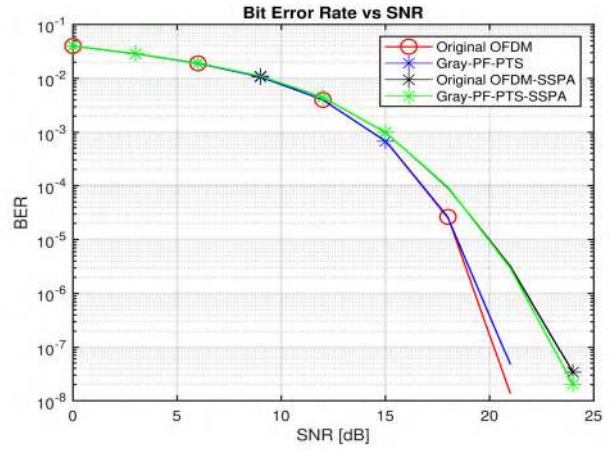

FIGURE 12. BER of the Gray-PF-PTS A algorithm in OFDM with and without SSPA, $N = 4096$, $M = 64$.

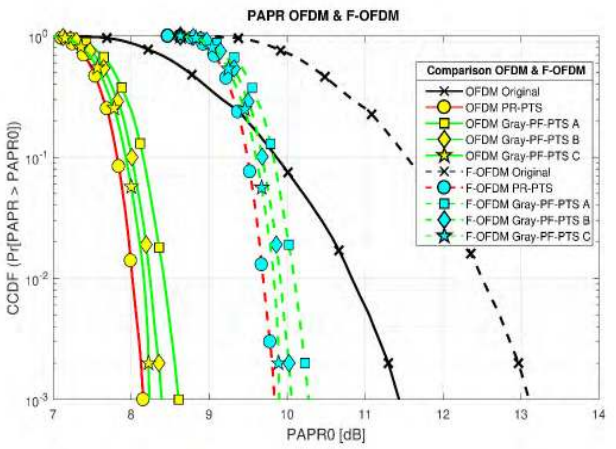

FIGURE 13. Comparison of the PAPR performances for the original signal, PR-PTS, and Gray-PF-PTS algorithms based on OFDM and F-OFDM, $N = 512$, $M = 256$.

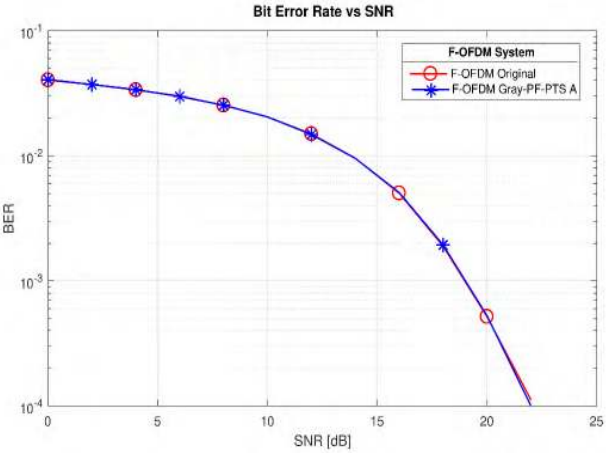

FIGURE 14. BER of the Gray-PF-PTS algorithm in F-OFDM, $N = 512$, $M = 256$.

leads to reducing the computational complexity significantly. Again, the Gray-PF-PTS A algorithm maintains the BER performance without degradation compared with the original OFDM signal, as shown in Figure 11. In addition, the comparison of the BER performance between the Gray-PF-PTS A algorithm with and without SSPA model is coeducated in Figure 12. It is clear that the nonlinearity exhibit of the SSPA model influences to the OFDM signal and leads to degradation in the BER performance.

In the F-OFDM system, a comparison between the Gray-PF-PTS algorithms and the PR-PTS method based on the OFDM and F-OFDM systems is conducted. The parameters for this simulation are: $N = 512$, $M = 256$, $V = 4$, $L = 4$, $W = 4$, CP $= 144$, $FL = 1025$, and $\alpha = 0.6$. Figure 13 illustrates the PAPR reduction performance for various algorithms, where the PAPR value based on OFDM is 8.15 dB, 8.23 dB, 8.39 dB, 8.6 dB, and 11.43 dB for PR-PTS, Gray-PF-PTS C, Gray-PF-PTS B, Gray-PF-PTS A, and the original signal, respectively. Moreover, the PAPR value based on F-OFDM is 9.83 dB, 9.9 dB, 10.06 dB, 10.27 dB, and 13.1 dB for PR-PTS, Gray-PF-PTS C, Gray-PF-PTS B, Gray-PF-PTS A, and the original signal, respectively. It is evident that the PAPR reduction performances of the algorithms based on OFDM are superior to the same schemes based on F-OFDM by 1.68 dB because the transmitter filter increases the gap between the peak power and mean power of the signal. Furthermore, the BER performances of the Gray-PF-PTS A scheme is compared with the original F-OFDM signal, where the BER performances for both signals are identical, as shown in Figure 14.

Besides, the comparison in terms of the BER performance between the Gray-PF-PTS A based on OFDM and the same algorithm based on F-OFDM is plotted in Figure 15. The probability of error in Gray-PF-PTS A based on F-OFDM is 1.9×10^{-3} and 5.27×10^{-4} at 18 dB and 20 dB of SNR, respectively, while the BER value of Gray-PF-PTS A based on OFDM is 4.33×10^{-3} and 1.5×10^{-3} at 18 dB and 20 dB of SNR, respectively. It is clear that the Gray-PF-PTS

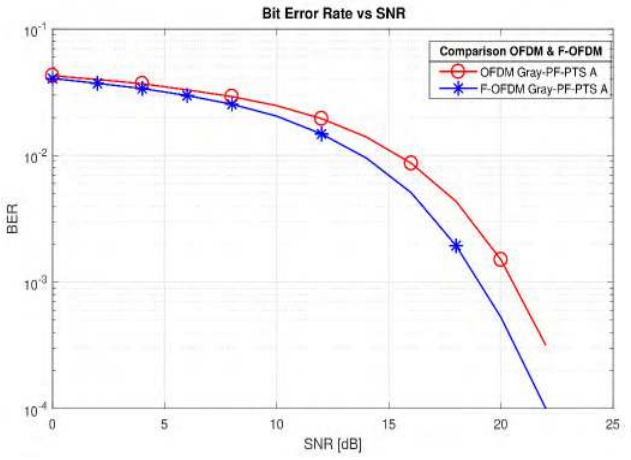

FIGURE 15. BER of Gray-PF-PTS A based on OFDM and F-OFDM, $N = 512$, $M = 256$.

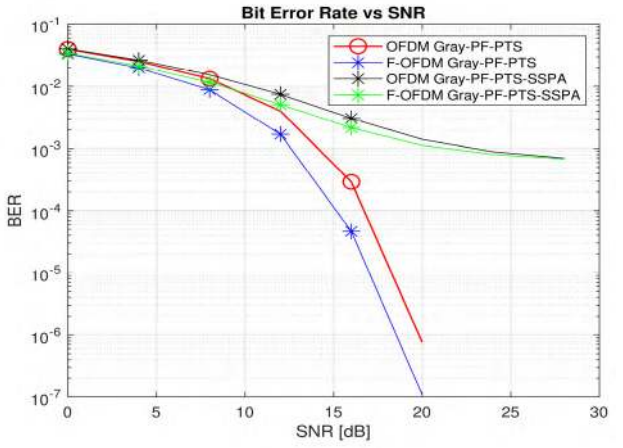

FIGURE 16. BER of Gray-PF-PTS A based on OFDM and F-OFDM with and without SSPA, $N = 512$, $M = 64$.

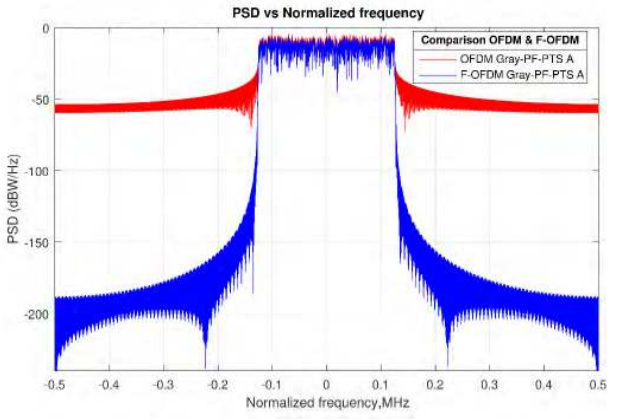

FIGURE 17. Comparison of the PSD performance for the Gray-PF-PTS A based on OFDM and F-OFDM systems, $N = 512$, $M = 256$.

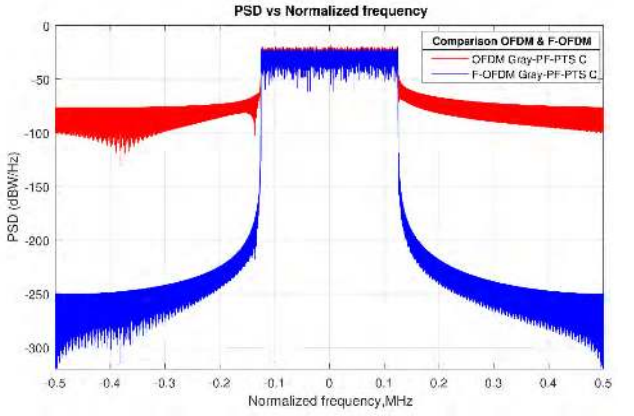

FIGURE 18. Comparison of the PSD performance for the Gray-PF-PTS C based on OFDM and F-OFDM systems, $N = 4096$, $M = 16$.

A algorithm based on F-OFDM has better BER performance than the same algorithm based on OFDM. This gain in the BER performance is due to the filtering operation, where the transmitter filter works to remove the sidelobes of the OFDM signal; thus, the interference between the symbols is reduced. Also, Figure 16 presents the BER performance of the proposed algorithm based on OFDM and F-OFDM. It can be seen that the SSPA model leads to degradation the BER performance compared with the system without SSPA model. Also, it is noted that the BER performances for the proposed algorithm with SSPA model suffer from error floors that appear at high SNRs, which are due to the nonlinear effect of the SSPA [50].

B. PSD EVALUATION

In this subsection, the PSD performance of the transmitted signal based on the OFDM and F-OFDM systems has been evaluated. Figure 17 illustrates the PSD shape comparison of the Gray-PF-PTS based on OFDM system and the same algorithm based on F-OFDM when $N = 512$ and $M = 256$. The result indicates that the OOBE of the Gray-PF-PTS A algorithm starts at -28.78 dB for OFDM, while the same algorithm starts at -94.62 dB for F-OFDM. Hence, the enhancement in PSD performance is 65.84 dB by applying the F-OFDM system. Another example is conducted when $N = 4094$ and $M = 64$, as shown in Figure 18. It is clear that the enhancement in PSD performance is 109.8 dB for the Gray-PF-PTS C based on F-OFDM. This advantage of the F-OFDM system is because the transmitter filter suppresses the OOBE leakage of the OFDM signal.

C. COMPUTATIONAL COMPLEXITY EVALUATION

The computational complexity here represents the number of complex addition and multiplication operations in the time-domain. In this subsection, the mathematical calculation of the Gray-PF-PTS algorithms will be calculated and compared with the PR-PTS method and some of the related methods that were presented in the literature. Table 10 records the time-domain equations of the complex addition and multiplication operations for C-PTS based

TABLE 10. Complexity equations of Gray-PF-PTS, PR-PTS, and some of the previously suggested methods in the time-domain.

Method	C_{add}	C_{mult}
PR-PTS	$W^{V-1}\times N\times(V-1)$	$W^{V-1}\times N\times(V+1)$
Gray-PF-PTS A	$2^{V-1}\times V\times N$	$2^{V-1}\times\left(\frac{V}{2}+3\right)\times N$
Gray-PF-PTS B	$2\left[2^{V-1}\times V\times N\right]-2N$	$2\left[2^{V-1}\left(\frac{V}{2}+3\right)\times N\right]-3N$
Gray-PF-PTS C	$3\left[2^{V-1}\times V\times N\right]-4N$	$3\left[2^{V-1}\left(\frac{V}{2}+3\right)\times N\right]-7N$
Lan-xun [23]	$I\times N\times(V-1)$	$I\times N\times(V+1)$
Liu [22]	$I\times N\times(V-1)$	$I\times N\times(V+1)$
Jayalath [24]	$I\times N\times(V-1)$	$I\times N\times(V+1)$
Jayalath [26]	$W^{V/2}\times N\times(V-1)$	$\left[W^{V/2}\times N\times\left(\frac{V}{2}+1\right)\right]$
Sarawong [27]	$W^{V-1}\times N\times(V-1)$	$W^{V-1}\times N\times(V+1)$
Kim [25]	$H\times N\times(V-1)$	$(H\times N)+[\,(H-1)\times(V-1)\times N\,]$
L. Wang [28]	$\left[W^{V/2}\times N\times(V-1)\right]\times(SS+1)$	$\left[W^{V/2}\times N\times\left(\frac{V}{2}+SS+1\right)\right]+(SS\times N)$
L. Wang [29]	$\left[W^{V/2}\times N\times(V-1)\right]\times(SSCP+1)$	$\left[W^{V/2}\times N\times\left(\frac{V}{2}+SSCP+1\right)\right]+(SSCP\times N)$
L. Wang [21]	$W^{V-1}\times N\times\left(\frac{V}{4}+1\right)$	$W^{V-1}\times N\times\left(\frac{V}{4}+1\right)$
Junjun [30]	$W^{V-1}\times N\times\frac{V}{2}$	$W^{V-1}\times N\times\left(\frac{V}{4}+1\right)$

TABLE 11. Computational complexity of Gray-PF-PTS and the various improved PTS methods in the literature, V = 4, W = 4.

N	PR-PTS		Gray-PF-PTS A		Gray-PF-PTS B		Gray-PF-PTS C		Lan-xun [23] I=12		Liu [22] I = 32		Jayalath [24] I = 38	
	C_{add}	C_{mult}	C_{add}	C_{mult}	C_{add}	C_{mult}	C_{add}	C_{mult}	C_{add}	C_{mult}	C_{add}	C_{mult}	C_{add}	C_{mult}
64	12288	20480	2048	2560	3968	4928	5888	7232	2304	3840	6144	10240	7296	12160
128	24576	40960	4096	5120	7936	9856	11776	14464	4608	7680	12288	20480	14592	24320
256	49152	81920	8192	10240	15872	19712	23552	28928	9216	15360	24576	40960	29184	48640
512	98304	163840	16384	20480	31744	39424	47104	57856	18432	30720	49152	81920	58368	97280
1024	196608	327680	32768	40960	63488	78848	94208	115712	36864	61440	98304	163840	116736	194560
2048	393216	655360	65536	81920	126976	157696	188416	231424	73728	122880	196608	327680	233472	389120
4096	786432	1310720	131072	163840	253952	315392	376832	462848	147456	245760	393216	655360	466944	778240

N	Jayalath [26]		Sarawong [27]		Kim [25]		Wang [28]		Wang [29]		Wang [21]	
	C_{add}	C_{mult}	C_{add}	C_{mult}	C_{add}	C_{mult}	C_{add}	C_{mult}	C_{add}	C_{mult}	C_{add}	C_{mult}
64	3072	3072	12288	20480	12288	16192	6144	4160	12288	6336	8192	8192
128	6144	6144	24576	40960	24576	32384	12288	8320	24576	12672	16384	16384
256	12288	12288	49152	81920	49152	64768	24576	16640	49152	25344	32768	32768
512	24576	24576	98304	163840	98304	129536	49152	33280	98304	50688	65536	65536
1024	49152	49152	196608	327680	196608	259072	98304	66560	196608	101376	131072	131072
2048	98304	98304	393216	655360	393216	518144	196608	133120	393216	202752	262144	262144
4096	196608	196608	786432	1310720	786432	1036288	393216	266240	786432	405504	524288	524288

on pseudo-random partitioning scheme, Gray-PF-PTS, and some of the improved PTS algorithms in the literature. The parameters that related to the computational complexity calculations are: the number of the subcarriers N = [64, 128, 256, 512, 1024, 2048, 4096], the number of subblocks $V = 4$, the number of elements for the phase rotation factor $W = 2$ and 4, the number of conjugated subblocks (SS) = 1, which related to Wang and Cao [28], the number of special

TABLE 12. Side information bits of Gray-PF-PTS and the various improved PTS methods in the literature, V = 4, W = 4.

$W = 4$, $V = 4$													
Method	PR-PTS	Gray-PF-PTS A	Gray-PF-PTS B	Gray-PF-PTS C	Lan-xun [23] I=12	Liu [22] I = 32	Jayalath [24] I = 38	Jayalath [26]	Sarawong [27]	Kim [25]	Wang [28]	Wang [29]	Wang [21]
SI	6	4	4	4	4	5	6	4	6	6	5	6	6

subblocks circular permutation ($SSCP$) = 3 which relates to Wang's method [29], the determination value (alfa) = 0.5 which relates to Sarawong's method [27], the number of shift sets (H) = 64 which relates to Kim's method [25], the number of iterations (I) which is related to the Jayalath algorithm [24], Liu algorithm [22], and Lan-xun algorithm [23]. For simplicity, we ignore the dependence on the oversampling factor L and the number of cyclic prefixes CP for all equations. Also, it is important to mention that the equations represent the time-domain complexity of the transmitter side based on the PTS technique in the OFDM system.

Table 11 records the number of complex addition and multiplication operations for the various algorithms in Table 10. In case of $W = 4$, the number of complex additions for the Gray-PF-PTS C has been reduced by 52.08%, 4.16%, 14.29%, and 28.12% compared with PR-PTS or Sarawong *et al.* [27] or Kim [25] or Wang and Liu [29], Liu *et al.* [22] or Wang and Cao [28], Jayalath and Telebureau [24], and Wang and Liu [21], respectively. However, the number of complex multiplications for Gray-PF-PTS C algorithm has been reduced by 64.37%, 28.75%, 40%, and 10.93% compared with PR-PTR or Sarawong *et al.* [27], Liu *et al.* [22], Jayalath and Telebureau [24], Wang and Liu [21], respectively. Also, Figure 19 and Figure 20 depicts the complex additions and multiplications levels of the Gray-PF-PTS algorithms compared with the other algorithms in the literature. The results show that the Gray-PF-PTS A algorithm has the lowest computational complexity among the algorithms in Table 11. Moreover, the Gray-PF-PTS B and Gray-PF-PTS C algorithms outperforms the other algorithms except for the complexity of Lan-xun's algorithm [23] and Jayalath's algorithm [26]; with the consideration that the proposed algorithms exceed Lan-xun's algorithm and Jayalath's algorithm regarding the PAPR reduction performance significantly, as shown in Figure 7 and 10. The enhancement in the computational complexity level of the Gray-PF-PTS A is due to exploiting the relationship nature among the Gray code strings to reduce the number of addition and multiplication operations for finding the optimum phase rotation factors.

On the other hand, Table 12 lists the side information bits required for the various algorithms in this subsection. Another advantage of the Gray-PF-PTS algorithms related to transferring the side information bits to the receiver was found. It is only necessary to transfer the Gray code index to the receiver which can produce the phase rotation factor of the three types of the Gray-PF-PTS algorithms. It is clear that the Gray-PF-PTS algorithms required 4 bits as side information compared with 5 bits for Liu *et al.* [22] and Wang and Cao [28], and 6 bits for the other algorithms with the consideration that the number of $W = 4$. Therefore, the Gray-PF-PTS algorithms can be considered better than other algorithms in terms of side information level.

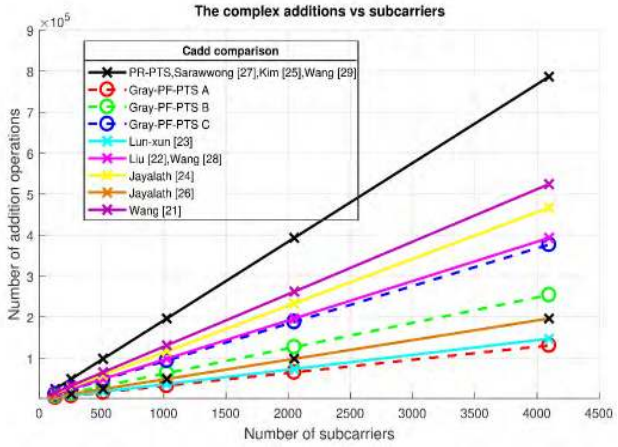

FIGURE 19. Comparison of the number of complex additions for various algorithms in Table 11.

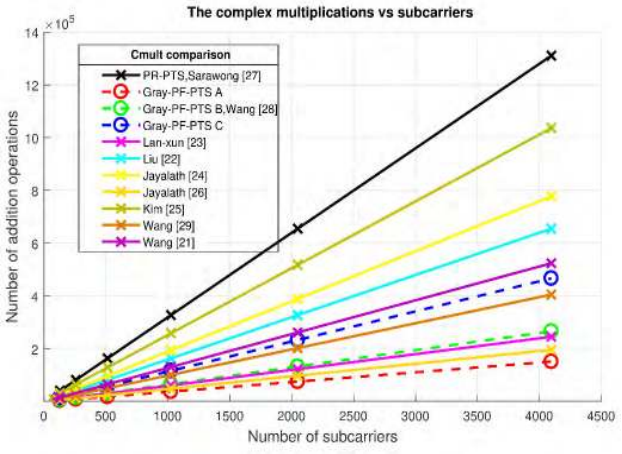

FIGURE 20. Comparison of the number of complex multiplications for various algorithms in Table 11.

As a result, the Gray-PF-PTS algorithm reduces the computational complexity level and the side information level extensively compared with the C-PTS method without degradation in the PAPR reduction performance. Therefore, the Gray-PF-PTS algorithm can be used to improve the PAPR reduction performance with low computational complexity and side information in the OFDM and F-OFDM systems

VI. CONCLUSION

In this study, the time domain computational complexity level in the PTS technique is significantly reduced by applying a new algorithm to the OFDM and F-OFDM systems. The Gray-PF-PTS algorithm is proposed relies on employing the Gray code with the Left Feedback Shift Register operation through a specific mapping rule to generate the phase rotation factors of the PTS technique. The scope of phase factor in Gray-PF-PTS is $\{\pm 1, \pm j\}$ with linear implementation, and the algorithm is expanded into three algorithms A, B, and C in order to enhance the PAPR reduction gain in OFDM and F-OFDM systems. The results indicate that the PAPR reduction performance of the Gray-PF-PTS C algorithm is almost the same as the conventional PR-PTS method, while the proposed algorithm is reduced the additions and multiplications operations by 52.06% and 64.37% compared with the PR-PTS method. Also, the number of side information bits of the proposed algorithm has been reduced by 33.33% compared with the conventional PTS method. Therefore, Gray-PF-PTS C can be deemed an efficient algorithm for enhancing the PAPR reduction capacity with low computational complexity and side information level in both OFDM and F-OFDM systems.

REFERENCES

[1] S. Ahmed and L. Zhang, "Complexity reduced detection for MIMO–OFDMA uplink with distinct frequency offsets from each user," *Phys. Commun.*, vol. 9, pp. 125–134, Dec. 2013.

[2] N. Ta pınar and Y. T. Bozkurt, "PAPR reduction using genetic algorithm in lifting-based wavelet packet modulation systems," *Turkish J. Elect. Eng. Comput. Sci.*, vol. 24, no. 1, pp. 184–195, 2016.

[3] Y. A. Jawhar, R. A. Abdulhasan, and K. N. Ramli, "A new hybrid sub-block partition scheme of PTS technique for reduction PAPR performance in OFDM system," *ARPN J. Eng. Appl. Sci.*, vol. 11, pp. 3904–3910, Apr. 2016.

[4] A. Singh and H. Singh, "Peak to average power ratio reduction in OFDM system using hybrid technique," *Optik*, vol. 127, no. 6, pp. 3368–3371, Mar. 2016.

[5] Y. A. Jawhar, R. A. Abdulhasan, and K. N. Ramli, "Influencing parameters in peak to average power ratio performance on orthogonal frequency-division multiplexing system," *ARPN J. Eng. Appl. Sci.*, vol. 11, no. 6, pp. 4322–4332, 2016.

[6] N. B. Raja and A. Gangatharan, "A new low complexity DHT based weighted OFDM transmission for peak power reduction," *Indian J. Sci. Technol.*, vol. 9, no. 17, pp. 1–4, 2016.

[7] B.-S. P. Lin, W.-H. Tsai, C. C. Wu, P. H. Hsu, J. Y. Huang, and T.-H. Liu, "The design of cloud-based 4G/LTE for mobile augmented reality with smart mobile devices," in *Proc. 7th IEEE Inter. Conf. Service-Oriented Syst. Eng.*, Redwood City, USA, Mar. 2013, pp. 561–566.

[8] N. Ta pınar and Y. T. Bozkurt, "Peak-to-average power ratio reduction using backtracking search optimization algorithm in OFDM systems," *Turkish J. Elect. Eng. Comput. Sci.*, vol. 24, no. 4, pp. 2307–2316, 2016.

[9] Y. A. Jawhar, K. N. Ramli, M. A. Taher, N. S. M. Shah, L. Audah, M. S. Ahmed, and T. Abbas, "New low-complexity segmentation scheme for the partial transmit sequence technique for reducing the high PAPR value in OFDM systems," *ETRI J.*, vol. 40, no. 6, pp. 1–15, Sep. 2018.

[10] P. P. Kumar and K. K. Kishore, "BER and PAPR analysis of UFMC for 5G communications," *Indian J. Sci. Technol.*, vol. 9, pp. 1–6, Dec. 2016.

[11] A. Osseiran, F. Boccardi, V. Braun, K. Kusume, P. Marsch, M. Maternia, O. Queseth, M. Schellmann, H. Schotten, H. Taoka, H. Tullberg, M. A. Uusitalo, B. Timus, and M. Fallgren, "Scenarios for 5G mobile and wireless communications: The vision of the METIS project," *IEEE Commun. Mag.*, vol. 52, no. 5, pp. 26–35, May 2014.

[12] X. Wang, T. Wild, and F. Schaich, "Filter optimization for carrier-frequency- and timing-offset in universal filtered multi-carrier systems," in *Proc. 81st IEEE 81st Veh. Technol. Conf.*, Glasgow, U.K., May 2015, pp. 1–6.

[13] L. Zhang, A. Ijaz, P. Xiao, A. Quddus, and R. Tafazolli, "Subband filtered multi-carrier systems for multi-service wireless communications," *IEEE Trans. Wireless Commun.*, vol. 16, no. 3, pp. 1893–1907, Mar. 2017.

[14] R. Gerzaguet, N. Bartzoudis, L. G. Baltar, V. Berg, J.-B. Doré, D. Kténas, O. Font-Bach, X. Mestre, M. Payaró, M. Färber, and K. Roth, "The 5G candidate waveform race: A comparison of complexity and performance," *EURASIP J. Wireless Commun. Netw.*, vol. 13, pp. 1–14, Dec. 2017.

[15] L. Zhang, A. Ijaz, P. Xiao, M. M. Molu, and R. Tafazolli, "Filtered OFDM systems, algorithms, and performance analysis for 5G and beyond," *IEEE Trans. Commun.*, vol. 66, no. 3, pp. 1205–1218, Mar. 2018.

[16] M. Taher, J. Mandeep, M. Ismail, S. Samad, and T. Islam, "Reducing the power envelope fluctuation of OFDM systems using side information supported amplitude clipping approach," *Int. J. Circuit Theory Appl.*, vol. 42, no. 4, pp. 425–435, 2014.

[17] K. Anoh, B. Adebisi, M. Rabie, and C. Tanriover, "Root-based nonlinear companding technique for reducing PAPR of precoded OFDM signals," *IEEE Access*, vol. 6, pp. 4618–4629, 2018.

[18] Z. Zheng and G. Li, "An efficient FPGA design and performance testing of the ACE algorithm for PAPR reduction in DVB-T2 systems," *IEEE Trans. Broadcast.*, vol. 63, no. 1, pp. 134–143, Mar. 2017.

[19] M. A. Taher, M. J. Singh, M. Ismail, S. A. Samad, and M. T. Islam, "Sliding the SLM-technique to reduce the non-linear distortion in OFDM systems," *Elektron. Elektrotechn.*, vol. 19, no. 5, pp. 103–111, 2014.

[20] Y. A. Al-Jawhar, N. S. M. Shah, M. A. Taher, M. S. Ahmed, and K. N. Ramli, "An enhanced partial transmit sequence segmentation schemes to reduce the PAPR in OFDM systems," *Int. J. Adv. Comput. Sci. Appl.*, vol. 7, no. 12, pp. 66–75, 2017.

[21] L. Wang and J. Liu, "PAPR reduction of OFDM signals by PTS with grouping and recursive phase weighting methods," *IEEE Trans. Broadcast.*, vol. 57, no. 2, pp. 299–306, Jun. 2011.

[22] P. Liu, W.-P. Zhu, and M. O. Ahmad, "A phase adjustment based partial transmit sequence scheme for PAPR reduction," *Circuits, Syst. Signal Process.*, vol. 23, no. 4, pp. 329–337, Aug. 2004.

[23] L.-X. Wang and L.-B. Yang, "A modified PTS method using m sequences for PAPR reduction," in *Proc. IEEE Int. Conf. Meas., Inf. Control*, Harbin, China, May 2012, pp. 837–840.

[24] A. D. S. Jayalath and C. Tellambura, "Adaptive PTS approach for reduction of peak-to-average power ratio of OFDM signal," *Electron. Lett.*, vol. 36, no. 14, pp. 1226–1228, Jul. 2000.

[25] K.-H. Kim, "On the shift value set of cyclic shifted sequences for PAPR reduction in OFDM systems," *IEEE Trans. Broadcast.*, vol. 62, no. 2, pp. 496–500, Jun. 2016.

[26] A. D. S. Jayalath, C. Tellambura, and H. Wu, "Reduced complexity PTS and new phase sequences for SLM to reduce PAP of an OFDM signal," in *Proc. IEEE 51st Veh. Technol. Conf.*, Tokyo, Japan, May 2000, pp. 1914–1917.

[27] J. Sarawong, T. Mata, P. Boonsrimuang, and H. Kobayashi, "Interleaved partitioning PTS with new phase factors for PAPR reduction in OFDM systems," in *Proc. 8th Elect. Eng./ Electron., Comput., Telecommun. Inf. Technol. (ECTI) Conf.*, Khon Kaen, Thailand, May 2011, pp. 361–364.

[28] L. Wang and Y. Cao, "Sub-optimum PTS for PAPR reduction of OFDM signals," *Electron. Lett.*, vol. 44, no. 15, pp. 921–922, Jul. 2008.

[29] L. Wang and J. Liu, "Cooperative PTS for PAPR reduction in MIMO-OFDM," *IEEE Electron. Lett.*, vol. 47, no. 5, pp. 351–352, Mar. 2011.

[30] J. Liu, Z. Wei, Y. Zhu, and M. Teng, "Low complexity PTS algorithm based on gray code and its FPGA implementation," in *Proc. IEEE 10th Int. Conf. Electron. Meas. Instrum.*, Chengdu, China, Aug. 2011, pp. 208–211.

[31] Y. A. Jawhar, N. S. Shah, M. A. Taher, M. S. Ahmed, K. N. Ramli, and R. Abdulhasan, "A low PAPR performance with new segmentation schemes of partial transmit sequence for OFDM systems," *Int. J. Adv. Appl. Sci.*, vol. 4, no. 4, pp. 14–21, 2017.

[32] Q. Bodinier, F. Bader, and J. Palicot, "Coexistence of filter banks and CP-OFDM: What are the real gains?" in *Proc. IEEE Int. Symp. Wireless Commun. Syst. (ISWCS)*, Poznan, Poland, Sep. 2016, pp. 628–632.

[33] K. Mhatre and U. P. Khot, "Efficient selective mapping PAPR reduction technique," *Procedia Comput. Sci.*, vol. 45, pp. 620–627, Mar. 2015.

[34] K. Ramli, M. Taher, L. Audah, N. S. Shah, M. Ahmed, and A. Hammoodi, "An enhanced partial transmit sequence based on combining Hadamard matrix and partitioning schemes in OFDM systems," *Int. J. Integr. Eng.*, vol. 10, no. 3, pp. 1–7, Jul. 2018.

[35] Y. Liu, X. Chen, Z. Zhong, B. Ai, D. Miao, Z. Zhao, J. Sun, Y. Teng, and H. Guan, "Waveform design for 5G networks: Analysis and comparison," *IEEE Access*, vol. 5, pp. 19282–19292, 2017.
[36] P. Weitkemper, J. Bazzi, K. Kusume, A. Benjebbour, and Y. Kishiyama, "Adaptive filtered OFDM with regular resource grid," in *Proc. IEEE Int. Conf. Commun. Workshops (ICC)*, Kuala Lumpur, Malaysia, May 2016, pp. 462–467.
[37] J. Wang, A. Jin, D. Shi, L. Wang, H. Shen, D. Wu, L. Hu, L. Gu, L. Lu, Y. Chen, J. Wang, Y. Saito, A. Benjebbour, and Y. Kishiyama, "Spectral efficiency improvement with 5G technologies: Results from field tests," *IEEE J. Sel. Areas Commun.*, vol. 35, no. 8, pp. 1867–1875, Aug. 2017.
[38] X. Zhang, M. Jia, L. Chen, J. Ma, and J. Qiu, "Filtered-OFDM—Enabler for flexible waveform in the 5th generation cellular networks," in *Proc. IEEE Int. Conf. Global Commun. Conf. (GLOBECOM)*, San Diego, CA, USA, Dec. 2015, pp. 1–6.
[39] P. Guan, D. Wu, T. Tian, J. Zhou, X. Zhang, L. Gu, A. Benjebbour, M. Iwabuchi, and Y. Kishiyama, "5G field trials: OFDM-based waveforms and mixed numerologies," *IEEE J. Sel. Areas Commun.*, vol. 35, no. 6, pp. 1234–1243, Jun. 2017.
[40] F. Schaich and T. Wild, "Waveform contenders for 5G—OFDM vs. FBMC vs. UFMC," in *Proc. 6th IEEE Int. Conf. Commun., Control Signal Process. (ISCCSP)*, May 2014, pp. 457–460.
[41] Y. A. Jawhar, L. Audah, M. A. Taher, K. N. Ramli, N. S. M. Shah, M. Musa, and M. S. Ahmed, "A review of partial transmit sequence for PAPR reduction in the OFDM systems," *IEEE Access*, vol. 7, pp. 18021–18041, 2019.
[42] S. H. Han and J. H. Lee, "PAPR reduction of OFDM signals using a reduced complexity PTS technique," *IEEE Signal Process. Lett.*, vol. 11, no. 11, pp. 887–890, Nov. 2004.
[43] Y. A. Al-Jawhar, K. N. Ramli, M. S. Ahmed, R. Abdulhasan, H. Farhood, and M. Alwan, "A New Partitioning Scheme for PTS Technique to Improve the PAPR Performance in OFDM Systems," *Int. J. Eng. Technol. Innov.*, vol. 8, no. 3, pp. 217–227, May 2018.
[44] S.-J. Ku, C.-L. Wang, and C.-H. Chen, "A reduced-complexity PTS-based PAPR reduction scheme for OFDM systems," *IEEE Trans. Wireless Commun.*, vol. 9, no. 8, pp. 2455–2460, Aug. 2010.
[45] K. Tani, Y. Medjahdi, H. Shaiek, R. Zayani, and D. Roviras, "PAPR reduction of post-OFDM waveforms contenders for 5G & Beyond using SLM and TR algorithms," in *Proc. 25th IEEE Int. Conf. Telecommun. (ICT)*, St. Malo, France, Jun. 2018, pp. 104–109.
[46] E. Agrell, J. Lassing, E. G. Strom, and T. Ottosson, "On the optimality of the binary reflected Gray code," *IEEE Trans. Inf. Theory*, vol. 50, no. 12, pp. 3170–3182, Dec. 2004.
[47] R. K. Driscoll, "Computer efficient linear feedback shift register," U.S. Patent 6 763 363 B1, Jul. 13, 2004.
[48] P. Kitsos, N. Sklavos, N. Zervas, and O. Koufopavlou, "A reconfigurable linear feedback shift register (LFSR) for the Bluetooth system," in *Proc. 8th IEEE Int. Conf. Electron., Circuits Syst. (ICECS)*, Malta, Sep. 2001, pp. 991–994.
[49] E. Al-Dalakta, A. Al-Dweik, A. Hazmi, C. Tsimenidis, and B. Sharif, "PAPR reduction scheme using maximum cross correlation," *IEEE Commun. Lett.*, vol. 16, no. 12, pp. 2032–2035, Dec. 2012.
[50] E. Al-Dalakta, A. Al-Dweik, A. Hazmi, C. Tsimenidis, and B. Sharif, "Efficient BER reduction technique for nonlinear OFDM transmission using distortion prediction," *IEEE Trans. Veh. Technol.*, vol. 61, no. 5, pp. 2330–2336, Jun. 2012.

YASIR AMER AL-JAWHAR received the B.S. degree in electrical engineering from the College of Engineering, University of Al-Mustansiriya, Baghdad, Iraq, in 1998, and the M.S. degree in engineering from the Faculty of Electrical and Electronic Engineering, University Tun Hussein Onn Malaysia, Johor, Malaysia, in 2015, where he is currently pursuing the Ph.D. degree in communication engineering. He is also a Chief Engineer with the Iraqi Ministry of Communication, Baghdad. His main research interests are signal processing in communication, OFDM, PAPR reduction in multicarrier system, 5G waveform design, and wireless network.

KHAIRUN NIDZAM RAMLI received the B.S. degree in electrical engineering from the Institute of Science and Technology, The University of Manchester, Manchester, U.K., in 1997, the M.S. degree in engineering from University Kebangsaan Malaysia, Kula Lumpur, Malaysia, in 2004, and the Ph.D. degree for research in electromagnetic analysis from the University of Bradford, U.K., in 2011. Since 2011, he has been with the Faculty of Electrical and Electronic Engineering, University of Tun Hussein Onn Malaysia, Johor, Malaysia, where he is currently a Senior Lecturer. His current research interests include wireless technologies, antennas, electromagnetics, and engineering computing.

AIDA MUSTAPHA received the B.Sc. degree in computer science from Michigan Technological University, in 1998, the M.Sc. degree in computer science from UKM, Malaysia, in 2004, and the Ph.D. degree in artificial intelligence focusing on dialogue systems. She is currently the Deputy Dean of the Center for Research and Development (R&D), Universiti Tun Hussein Onn Malaysia. She is also an Active Researcher in computational linguistics, soft computing, data mining, and agent-based systems.

SALAMA A. MOSTAFA received the B.Sc. degree in computer science from the University of Mosul, Iraq, in 2003, and the M.Sc. and Ph.D. degrees in information technology from UNITEN, Malaysia, in 2011 and 2016, respectively. He is currently a Postdoctoral Staff with Universiti Tun Hussein Onn Malaysia, Malaysia. His research interests include soft computing, data mining, and intelligent autonomous systems.

NOR SHAHIDA MOHD SHAH received the B.S. degree in electrical engineering from the Tokyo Institute of Technology, Tokyo, Japan, in 2000, the M.S. degree from the University of Malaya, Kula Lumpur, Malaysia, in 2003, and the Ph.D. degree from Osaka University, Tokyo, in 2012. Since 2011, she has been with the Faculty of Electrical and Electronic Engineering, Universiti Tun Hussein Onn Malaysia, Johor, Malaysia, where she is currently a Senior Lecturer. Her current research interests include optical fiber devices, optical communication, nonlinear optics, optical signal processing, antenna and propagation, and wireless communication.

MONTADAR ABAS TAHER received the B.S. degree in electronics and communications engineering and the M.S. degree in satellite engineering from Al-Nahrain University, Baghdad, Iraq, in 2000 and 2003, respectively, and the Ph.D. degree from University Kebangsaan Malaysia, Kula Lumpur, Malaysia, in 2015. Since 2010, he has been with the Department of Communication, University of Diyala, Diyala, Iraq, where he is currently a Senior Lecturer. His current research interests include OFDM, CDMA, MC-CDMA, PAPR reduction in multicarrier systems, and DSP for telecommunication.